Polyhedron 48 (2012) 43–50

Contents lists available at SciVerse ScienceDirect

Polyhedron

journal homepage: www.elsevier.com/locate/poly

Oxidative DNA cleavage, cytotoxicity and antimicrobial studies of L-ornithine copper (II) complexes

P.R. Chetana [a,*], Ramakrishna Rao [a], Sounik Saha [b], R.S. Policegoudra [c], P. Vijayan [d], M.S. Aradhya [e]

[a] Department of Chemistry, Central College Campus, Bangalore University, Bangalore 560001, India
[b] Department of Inorganic & Physical Chemistry, Indian Institute of Science, Sir C.V. Raman Avenue, Bangalore 560012, India
[c] Department of Biotechnology, Defense Research Laboratory, Tezpur 784001, India
[d] JSS College of Pharmacy, Ooty 643001, India
[e] Department of Fruit and Vegetable Technology, CFTRI, Mysore 570020, India

ARTICLE INFO

Article history:
Received 19 May 2012
Accepted 6 August 2012
Available online 13 September 2012

Keywords:
Ornithine
Copper (II)
DNA cleavage
A-549
HEp-2
Antibacterial activity

ABSTRACT

New ternary copper (II) complexes, [Cu(L-orn)(B)(Cl)](Cl·2H_2O) (**1**–**2**) where L-orn is L-ornithine, B is an *N*,*N*-donor heterocyclic base, viz. 2,2′-bipyridine (bpy, **1**) and 1,10-phenanthroline (phen, **2**), were synthesized and characterized by various spectroscopic techniques. Complex **2** is characterized by the X-ray single crystallographic method. The complex shows a distorted square-pyramidal (4 + 1) CuN_3OCl coordination sphere. Binding interactions of the complexes with calf thymus DNA (CT-DNA) were investigated by UV–Vis absorption titration, ethidium bromide displacement assay, viscometric titration experiment and DNA melting studies. Complex **2** shows appreciable chemical nuclease activity in the presence of 3-mercaptopropionic acid (MPA). The complexes were subjected to *in vitro* cytotoxicity studies against carcinomic human alveolar basal epithelial cells (A-549) and human epithelial (HEp-2) cells. The IC_{50} values of **1** and **2** are less than that of cisplatin against HEp-2 cell lines. MIC values for **1** against the bacterial strains *Streptococcus mutans* and *Pseudomonas aeruginosa* are 0.5 mM.

1. Introduction

Metal complexes constitute a growing field in drug design and have been considered as promising antitumor agents in recent decades by the virtue of their unique spectroscopic and electrochemical signatures. The interest in the role of metal complexes in cancer therapy was triggered by the discovery of the potent epithelial ovarian cancer drug cisplatin [1]. Metal complexes with tunable coordination environments and versatile physicochemical properties offer scope for designing and developing highly sensitive diagnostic agents for medicinal applications [2–17]. Metal complexes with polypyridyl phenanthroline bases have attracted great attention by virtue of their binding propensity to nucleic acids under physiological conditions. In addition to the rich coordination chemistry of the metal ions, they have great potential in constructing metal complexes with diverse structures and redox potentials [18–22]. Coordination compounds of the bioessential element copper have been extensively used in metal mediated DNA cleavage through the generation of hydrogen abstracting activated oxygen species (ROS). Sigman et al. investigated the chemical nuclease activity of a bis-(1,10-phenanthroline) copper (I) complex, which on activation with H_2O_2 induced oxidative strand scission [2]. The active oxo species attack the deoxyribose sugar proton of the nucleotide, which is in the vicinity of the copper (I) bisphen species in the minor groove, oxidatively initiating a series of free radical chain reactions to induce DNA strand scission [23,24]. The strong binding affinity of the copper bis phen complex and the redox behavior of the copper center play an important role in inducing oxidative DNA cleavage. Chakravarty and co-workers recently explored amino acid transition metal based chemistry towards cleavage of DNA under physiological conditions by oxidative as well as photochemical means on charge transfer or d–d band excitation [25–39]. The copper complex of L-lysine structure is closely resembles the copper–ornithine structure, which shows efficient chemical nuclease activity [25]. The present work stems from our interest to explore chemical nuclease activity, cytotoxicity against A-549 and HEp-2 cancer cells and antimicrobial activities of L-ornithine copper (II) complexes.

Compounds with α-amino acids containing a terminal amine moiety easily penetrate through cell walls due to their ionic character. L-Ornithine is a non-protein, basic amino acid and it is most potent for stimulating, production and release of growth hormones, in maintaining arterial flexibility and defeating hypertension [40–42]. Ornithine decarboxylase activity is higher in rapidly growing tumors than in non-malignant tumors [43–45]. This activity may be reduced by chelating the carboxylate group of ornithine. Due to these activities of L-ornithine, we were inter-

* Corresponding author. Tel./fax: +91 80 22961353.
E-mail address: pr.chetana@gmail.com (P.R. Chetana).

0277-5387/$ - see front matter © 2012 Elsevier Ltd. All rights reserved.
http://dx.doi.org/10.1016/j.poly.2012.08.081

ested in exploring the chemical nuclease activity of L-ornithine copper complexes.

Herein, we report the two new ternary copper (II) complexes [Cu(L-orn)(B)(Cl)](Cl·2H_2O) (**1**–**2**), where L-orn is L-ornithine, B is *N*,*N*-donor heterocyclic base, viz. 2,2′-bipyridine (bpy, **1**) and 1,10-phenanthroline (phen, **2**), which were synthesized and characterized by various spectroscopic techniques. Complex **2** is characterized by single X-ray crystallographic method. Studies have been made to explore the role of a DNA binder and amino acid with a terminal amine group along with the mechanistic pathways involved in the chemical nuclease activity.

2. Experimental

2.1. Materials and methods

The reagents and chemicals were purchased from commercial sources and used as received without further purification. The solvents used were purified by standard procedures [46]. Supercoiled (SC) pUC19 DNA (cesium chloride purified) was purchased from Bangalore Genie (India). CT-DNA, agarose (molecular biology grade), distamycin-A, catalase, superoxide dismutase (SOD) and ethidium bromide (EB) were from Sigma (USA). Tris(hydroxymethyl)aminomethane–HCl (Tris–HCl) buffer was prepared using deionized and sonicated triple distilled water. The elemental analysis was done using a Thermo Finnigan FLASH EA 1112 CHNS analyzer. The infrared and electronic spectra were recorded on Perkin Elmer Lambda 35 and Perkin Elmer spectrum one 55 spectrophotometers respectively at 25 °C. Magnetic susceptibility data for polycrystalline samples of the complexes were obtained using a Model 300 Lewis-coil-force magnetometer of George Associates Inc. (Berkeley, USA) make and Hg[$Co(NCS)_4$] was used as a standard. Experimental susceptibility data were corrected for diamagnetic contributions [47]. Molar conductivity measurements were carried out using a Control Dynamics (India) conductivity meter. Cyclic voltammetric measurements were made at 25 °C on a EG&G PAR 253 Versastat potentiostat/galvanostat using a three electrode configuration consisting of a glassy carbon working, a platinum wire auxiliary and a saturated calomel reference (SCE) electrode.

2.2. Synthesis

2.2.1. Preparation of [Cu(L-orn)(B)(Cl)](Cl) (**1**–**2**) (L-orn = L-ornithine and B = bpy, **1**; phen, **2**)

An aqueous solution of $CuCl_2·3H_2O$ (0.48 g, 2 mM) was reacted with L-ornithine which was pre-treated with NaOH (0.08 g, 2.0 mM) in water (10 mL) and stirred for 2 h at room temperature. A 20 mL methanolic solution of the heterocyclic base [bpy (0.28 g), phen (0.35 g)] was added dropwise using a syringe at room temperature. The solid that formed was filtered and the filtrate, on slow concentration, yielded a blue crystalline solid of the complexes (Scheme 1).

Anal. Calc. for $C_{15}H_{24}CuN_4O_4Cl_2$ (**1**): C, 39.23; H, 5.23; N, 12.20. Found: C, 39.64; H, 5.24; N, 12.73%. FT-IR, cm^{-1} (KBr disc): 3107br, 3051w, 1608s, 1560m, 1494m, 1471s, 1442vs, 1315s [br, broad; vs, very strong; s, strong; m, medium; w, weak]. UV–Vis in water [λ_{max}, nm (ε, M^{-1} cm^{-1})]: 312 (7590), 588 (75). Magnetic moment at 298 K [μ_{eff}/BM]: 1.56. Λ_M (Ω^{-1} cm^2 M^{-1}) in water at 25 °C: 143. ESI-MS in methanol *m*/*z*: 417.41 $[M-Cl]^+$.

Anal. Calc. for $C_{17}H_{24}CuN_4O_4Cl_2$ (**2**): C, 42.36; H, 4.99; N, 11.63. Found: C, 42.32; H, 4.94; N, 11.61%. FT-IR, cm^{-1} (KBr disc): 3252br, 3446br, 3247m, 3128w, 1172w, 1622vs, 1514m, 1421m, 848m, 721m. Magnetic moment at 298 K [μ_{eff}/BM]: 1.79. UV–Vis in water [λ_{max}, nm (ε, M^{-1} cm^{-1})]: 789 (13), 626 (72), 610 (65), 376 (903), 232 (1356), 208 (1168). Λ_M (Ω^{-1} cm^2 M^{-1}) in water at 25 °C: 137. ESI-MS in methanol *m*/*z*: 443.44 $[M-Cl]^+$.

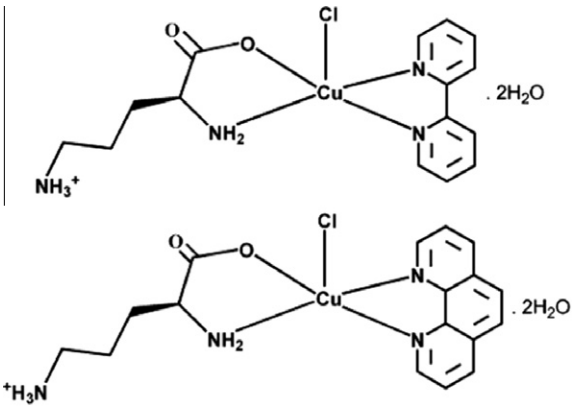

Scheme 1. Schematic representation of complexes **1** and **2**.

2.3. X-ray crystallographic procedures

Single crystals of **2** were grown by slow evaporation of water/methanol mixture. A block shaped single crystal was mounted on a glass fiber with epoxy cement. The X-ray diffraction data were measured in frames with increasing ω (width of 0.3° per frame) and with a scan speed of 15 s/frame on a Bruker SMART APEX CCD diffractometer, equipped with a fine focus 1.75 kW sealed tube X-ray source. Empirical absorption corrections were carried out using the multi-scan program [48]. The structure was solved by the heavy atom method and refined by full matrix least-squares using the SHELX system of programs [49]. All non-hydrogen atoms were refined anisotropically and the hydrogen atoms were refined isotropically. The hydrogen atoms attached to the hetero atoms were in their calculated positions and refined according to the riding model. The perspective view of the complex was obtained by ORTEP [50].

2.4. DNA binding and cleavage experiments

DNA binding experiments were performed in Tris–HCl/NaCl buffer (5 mM Tris–HCl, 5 mM NaCl, pH 7.2) using an aqueous solution of the complexes. CT-DNA (ca. 250 μM NP) in Tris–HCl buffer medium gave a ratio of the UV absorbances at 260 and 280 nm of ca.1.9:1, indicating the purity of DNA which is apparently free from protein [51]. The concentration of DNA was calculated from its absorption intensity at 260 nm with the known molar absorption coefficient value of 6600 M^{-1} cm^{-1} [52]. UV–Vis absorption titration experiments were performed by varying the concentration of CT-DNA keeping the metal complex concentration constant (50 μM) with due correction for the absorbance of CT-DNA itself. Samples were allowed to get equilibrated to bind sufficiently to CT-DNA before recording each spectrum. The intrinsic equilibrium binding constant (K_b) and the binding site size (*s*) of the complex were determined from a non-linear fitting of the plot of $\Delta\varepsilon_{af}/\Delta\varepsilon_{bf}$ versus [DNA] using the McGhee–von Hippel (MvH) method. The expression of Bard and coworkers: $\Delta\varepsilon_{af}/\Delta\varepsilon_{bf} = (b - (b^2 - 2K_b^2C_t[DNA]/s)^{1/2})/2K_b$, $b = 1 + K_bC_t + K_b[DNA]/2s$ was used to evaluate K_b and *s*, where K_b is the microscopic equilibrium binding constant for each site, C_t is the total concentration of the metal complex, *s* is the site size of the metal complex interacting with the DNA, [DNA] is the concentration of DNA in nucleotides, ε_f, ε_a and ε_b are respectively the molar extinction coefficients of the free complex in solution, complex bound to DNA at a definite concentration and the complex in the completely bound form with CT-DNA

[53,54]. The non-linear least-squares analysis was done using Origin Lab software, version 6.1.

The fluorescent spectral measurements were done using an ethidium bromide (EB) bound CT-DNA solution (260 μM) in 5 mM Tris–HCl buffer (pH 7.2) at 25 °C. EB itself did not show any fluorescence in Tris–HCl buffer medium as its fluorescence was quenched due to collision of EB with the excess solvent molecules [55,56]. EB showed enhanced fluorescence emission due to its intercalation to CT-DNA which make EB inaccessible to the solvent molecule. The fluorescent intensity of EB bound CT-DNA at 600 nm with increasing concentration of the complex was recorded. The addition of metal complex to CT-DNA could result in the competitive displacement of EB and hence a decrease in the emission intensity. The apparent binding constants (K_{app}) for the complexes were determined by using the equation: K_{app}[complex] = K_{EB}[EB] [57].

DNA-melting experiments were carried out by monitoring the absorbance of CT-DNA (260 nm) with increasing temperature in the absence and presence of the complexes in a molar ratio of 10:1 of the CT-DNA and the complex in phosphate buffer medium (pH 6.8) with a ramp rate of 0.5 °C min^{-1} using a Cary Bio UV–Vis spectrophotometer.

Viscometric titration experiments were performed using a Schott Gerate AVS310 automated viscometer that was thermostated at 37 (±0.1) °C in a constant temperature bath. The concentration of CT-DNA was 170 μM. The flow time was measured with an automated timer. The data were presented by plotting the relative specific viscosity of DNA, $(\eta/\eta_0)^{1/3}$ versus R, where η is the viscosity of DNA in the presence of the complex and η_0 is the viscosity of DNA alone in 5 mM Tris–HCl buffer medium, R = [complex]/[DNA]. The viscosity values were calculated from the observed flow time of CT-DNA containing solutions (t), duly corrected for that of the buffer alone (t_0), $\eta = (t - t_0)/t_0$.

The oxidative cleavage of SC pUC19 DNA by the ternary copper (II) complexes was studied by agarose gel electrophoresis. MPA (5 mM) was used as the reducing agent for the chemical nuclease activity. Reactions were carried out in the dark at 25 °C using SC DNA (1 μL, 0.2 μg 30 μM) in 50 mM Tris–HCl buffer (pH 7.2) containing 50 mM NaCl and the complexes (2 μL) with varied concentrations. The concentration of the complexes in DMF or the additives in buffer corresponded to the quantity after the dilution of the complex stock to the 20 μL final volume using Tris–HCl buffer. The SC pUC19 DNA samples were pre-incubated for 1 h at 37 °C, followed by its addition to the loading buffer containing 0.25% bromophenol blue, 0.25% xylene cyanol and 30% glycerol (2 μL) and the solution was finally loaded on 0.8% agarose gel containing 1.0 μg mL^{-1} ethidium bromide (EB). The electrophoresis experiment was carried out in a dark room for 2 h at 45 V in TAE (Tris–acetate–EDTA) buffer. The bands were visualized by UV light and photographed. The extent of cleavage of SC-DNA was determined by measuring the intensities of the bands using a UVITECH Gel Documentation System. Due corrections were made for the low level of nicked circular (NC) form present in the original SC-DNA sample and for the low affinity of EB binding to SC compared to NC and linear forms of DNA [58]. Different additives were added to the SC DNA for mechanistic investigations in the presence of the copper (II) complexes.

2.5. Cytotoxicity assay

Cell cultures were obtained from Christian Medical College, Vellore. A-549 cells and HEp-2 were grown in Dulbecco's Modified Eagle's Medium (DMEM) supplemented with 2 mM L-glutamine, 10% fetal bovine serum, penicillin (100 μg/mL), streptomycin (100 μg/mL) and amphoterecin B (5 μg/mL). The cells were maintained at 37 °C in a humidified atmosphere with 5% CO_2 and subcultured once a week. Sulforhodamine B (SRB) assay was conducted as per the reported procedures [59]. A-549 (human alveolar basal epithelial cells) cells are squamous in nature, responsible for the diffusion of substances such as water and electrolytes across the alveoli of lungs. HEp-2 cells resist temperature, nutritional and environmental changes without a loss of viability. They support the growth of arbo viruses and measles virus.

2.6. Antimicrobial activity

The antibacterial activity was tested against clinical isolates like *Bacillus subtilis*, *Micrococcus luteus*, *Staphylococcus aureus*, *Streptococcus mutans*, *Escherichia coli*, *Pseudomonas aeruginosa* and *Proteus vulgaris*. The test organisms were maintained on nutrient agar slants. *In-vitro* antibacterial activity was determined by the agar well-diffusion method as described by Mukherjee et al. [60]. The overnight bacterial culture was centrifuged at 8000 rpm for 10 min. The bacterial cells were suspended in saline to make a suspension of 105 CFU/mL and used for the assay. Plating was carried out by transferring the bacterial suspension to a sterile Petri plate, mixed with molten nutrient agar medium, and allowing the mixture to solidify. About 75 μL of the sample (2 mg/mL) was placed in the wells. Plates were incubated at 37 °C and activity was determined by measuring the diameter of the inhibition zones. The assay was carried out in triplicate. The MIC was determined according to the method described by Jones et al. [61]. Different concentrations of the compounds and 100 μL of the bacterial suspension (105 CFU/mL) were placed aseptically in 10 mL of nutrient broth separately and incubated for 24 h at 37 °C. Growth was observed at regular intervals followed by pour plating as described above. The lowest concentration of the test sample showing no visible growth was recorded as the MIC. Triplicate sets of tubes were maintained for each concentration of test sample.

3. Results and discussion

3.1. Synthesis and general properties

The complexes are one electron paramagnetic at room temperature, corresponding to d^9 electronic configuration for the copper (II) center. The complexes display a copper (II) centered d–d band at ~600 nm in addition to the ligand centered bands in the UV region of the electromagnetic spectra (Fig. 1). The electronic spectra of the complexes are in good agreement with the previously reported square pyramidal geometry of the complexes [36,37]. The complexes show a metal centered quasi-reversible

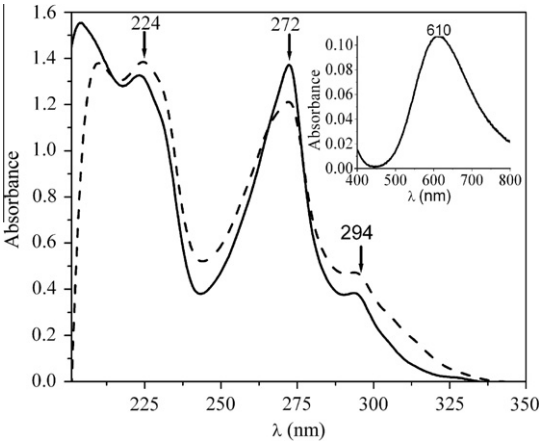

Fig. 1. The electronic spectra of complexes **1** (...) and **2** (—) in water, inset shows the d–d band of **2**.

cyclic voltammetric response due to the Cu(II)/Cu(I) couple near −0.5 V versus SCE in DMF 0.1 M TBAP.

3.2. Crystal structure

Complex **2** was structurally characterized by the single-crystal X-ray diffraction technique. It crystallized in the monoclinic $P2_1$ space group with two independent molecules in the crystallographic asymmetric unit and a goodness-of-fit 1.09. The unit cell packing contains two complex ions, $[Cu(L\text{-orn})(phen)(Cl)]^+$, four uncoordinated water molecules and two chloride ions. Selected crystallographic data are summarized in Table 1. The ORTEP view of **2** is shown in Fig. 2. Selected bond distances and angles are given in Table 2. The copper (II) complex displays a distorted (4 + 1) square-pyramidal geometry, in which Cu^{2+} coordinates with two nitrogen atoms of 1,10-phenanthroline, one nitrogen atom of an amino group, one carboxylate oxygen atom of L-ornithine in the equatorial positions and Cl^- at the elongated apical position. The configuration at the chiral α-carbon is *S* in the complex. The average trigonal distortion parameter (τ) value in the structure is 0.110. The average Cu–N1(phen), Cu–N2(phen), Cu–O(L-orn), Cu–N(L-orn) and Cu–Cl bond distances are 2.000(2), 2.052(2), 1.955(3), 2.015(2) and 2.542(11) Å, respectively. The alkyl chain of the cationic amino group $-(CH_2)_3NH_3^+$ remains as a pendant moiety. The X–Cu–Z angles are in the range 163.4(12)–156.76(12)°, where X and Z are any two atoms which lie trans to each other, and the X–Cu–Y angles range from 81.44(9)° to 101.52(10)°, where X and Y are any two atoms which lie cis to each other. The square pyramidal geometry around the central metal atom is severely distorted. The structure show extensive intermolecular non-covalent interactions. The water molecule is involved in hydrogen bonding interactions with the terminal cationic amine (NH_3^+) of L-ornithine. The terminal amine forms two H bonds with two lattice water molecules N(4)–Ow(1) and N(4)–Ow(2) (distances: 2.931 and 2.879 Å). The free oxygen atom of the carboxylate group of L-ornithine forms two H bonds, one with lattice water (O2–Ow2) and other with the lattice water of another asymmetric unit (O2–Ow(1)) with distances of 2.927 and 2.781 Å respectively. The Cl^- axial ligand is H bonded with the lattice water of another asymmetric unit with a distance of 3.238 Å. The lattice Cl^- is H bonded with latice water, Ow(1)–Cl(2), with a distance of 3.126 Å.

Table 1
Selected crystallographic data for **2**·$2H_2O$.

Empirical formula	$C_{17}H_{24}Cl_2CuN_4O_4$
Formula weight	482.84
Crystal system	monoclinic
Space group	$P2_1$
Unit cell dimensions	
a (Å)	10.2680(4)
b (Å)	6.7945(3)
c (Å)	14.9682(6)
β (°)	108.773(2)
V (Å^3)	988.72(7)
Z	2
T (K)	293(2)
ρ_{calc} (g cm^{-3})	1.622
λ (Å) (Mo Kα)	0.71073
μ (cm^{-1})	1.407
Data/restraints/parameters	2947/1/253
F(000)	498
Goodness-of-fit	1.09
R (F_o),[a] $I > 2\sigma(I)$/*wR*(F_o)[b]	0.0275/0.0774
R (all data)/*wR* (all data)	0.0295/0.0789
Largest difference in peak and hole (e Å^{-3})	0.440, −0.273

[a] $R = \Sigma||F_o| - |F_c||/\Sigma|F_o|$.
[b] $wR = \{\Sigma[w(F_o^2 - F_c^2)^2]/\Sigma[w(F_o)^2]\}^{1/2}$; $w = [\sigma^2(F_o)^2 + (AP)^2 + BP]^{-1}$, where $P = (F_o^2 + 2F_c^2)/3$, $A = 0.0480$, $B = 0.0341$ for **2**·$2H_2O$.

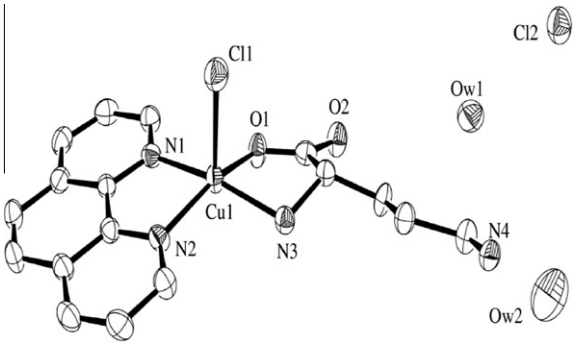

Fig. 2. ORTEP view of the complex $[Cu(L\text{-orn})(phen)(Cl)]Cl\cdot 2H_2O$ (**2**) showing thermal ellipsoids at the 50% probability level. The atom labeling scheme is shown for the metal ion and the heteroatoms. Hydrogen atoms and water molecules of crystallization are omitted for clarity.

Table 2
Selected bond distances (Å) and bond angels (°) for the complex $[Cu(L\text{-orn})(phen)(Cl)]Cl\cdot 2H_2O$ (**2**).

Cu(1)–N(1)	2.000(2)	N(1)–Cu(1)–Cl(1)	99.39(8)
Cu(1)–N(2)	2.052(2)	N(3)–Cu(1)–Cl(1)	96.34(9)
Cu(1)–N(3)	2.015(3)	N(2)–Cu(1)–Cl(1)	98.46(10)
Cu(1)–O(1)	1.955(2)	C(10)–N(2)–Cu(1)	130.2(2)
Cu(1)–Cl(1)	2.542(11)	C(1)–N(1)–Cu(1)	127.6(2)
O(1)–Cu(1)–N(1)	88.75(9)	C(12)–N(1)–Cu(1)	113.8(2)
O(1)–Cu(1)–N(3)	82.31(9)	O(1)–Cu(1)–Cl(1)	103.92(9)
N(1)–Cu(1)–N(3)	163.40(12)	N(1)–Cu(1)–Cl(1)	99.39(8)
O(1)–Cu(1)–N(2)	156.76(12)	O(1)–Cu(1)–Cl(1)	103.92(9)
N(1)–Cu(1)–N(2)	81.44(9)	N(1)–Cu(1)–Cl(1)	99.39(8)
N(3)–Cu(1)–N(2)	101.52(10)	N(2)–Cu(1)–Cl(1)	98.46(10)
O(1)–Cu(1)–Cl(1)	103.92(9)	N(3)–Cu(1)–Cl(1)	96.34(9)

3.3. DNA binding studies

The binding interactions of the complexes with CT-DNA have been investigated by absorption, emission spectroscopic, viscometric titration and DNA melting techniques. UV–Vis absorption spectral measurements were carried out to evaluate the equilibrium binding constant (K_b) and binding site size (*s*) of the complexes to CT-DNA by monitoring the change in the absorption intensity of the spectral band at ~300 nm for both complexes. Complex **2** showed a minor bathochromic shift of ~3 nm with significant hypochromism of 10–20%, suggesting mainly a groove binding propensity to the ds DNA (Fig. 3). The binding constant (K_b) and binding site size (*s*) values for **2** are 2.7 (±0.6) × 10^4 M^{-1} and 0.12 respectively. It shows an efficient DNA groove binding propensity. The bpy complex **1**, which lacks a planar aromatic system, displays a poor binding affinity to the double stranded CT-DNA. The binding site size (*s*), which is a measure of the number of DNA base pairs associated with the complex, suggests primarily a DNA groove-binding nature of the complex in preference to intercalation. The low value of *s* (⩽1) suggests surface aggregation of hydrophobic molecules on DNA due to π-stacking or an electrostatic interaction [62].

The emission spectral method is used to study the relative binding of the complexes to CT-DNA. The emission intensity of ethidium bromide (EB) is used as a spectral probe. EB shows reduced emission intensity in buffer solution because of solvent quenching and an enhancement of the emission intensity when intercalatively bound to DNA. The binding of the complexes to DNA decreases the emission intensity of EB. The relative binding propensity of the complexes to DNA is measured from the extent of reduction in the emission intensity (Fig. 4). The apparent binding constant (K_{app}) values for **1** and **2** are 0.68 × 10^5 and 1.6 × 10^5 M^{-1} respectively.

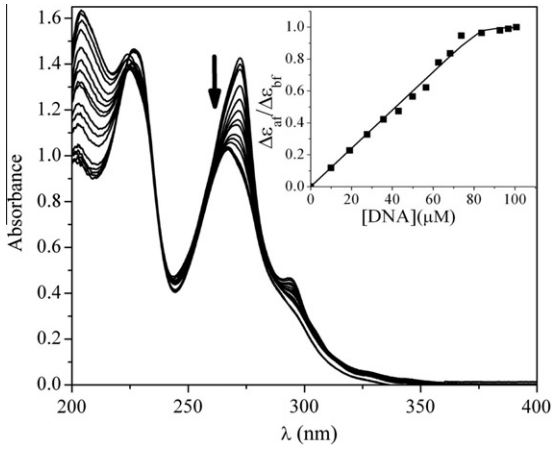

Fig. 3. Absorption spectral traces showing the decrease of absorption intensity on gradual addition of CT-DNA (250 μM, in aliquots to the solution of **2** (40 μM) in 5 mM Tris–HCl buffer (pH 7.2) at 25 °C. Inset shows the plot of $\Delta\varepsilon_{af}/\Delta\varepsilon_{bf}$ vs. [DNA].

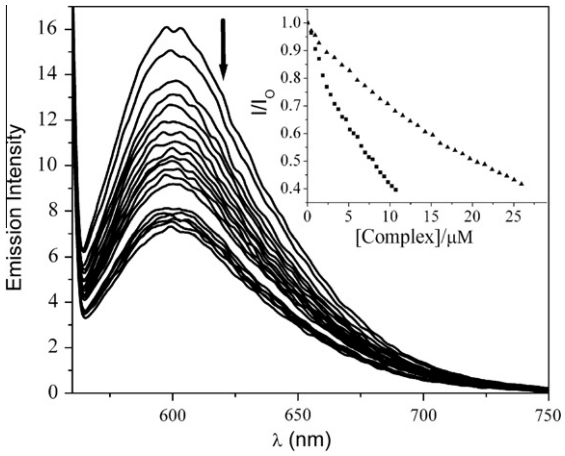

Fig. 4. Emission spectral changes on addition of **2** to CT-DNA bound to ethidium bromide (shown by arrow). Inset: Effect of addition of complex **1** (▲), **2** (■) to the emission intensity of CT-DNA-bound ethidium bromide in 5 mM Tris–HCl/5 mM NaCl buffer (pH 7.2) at 25 °C.

A viscometric titration experiment was carried out to explore the propensity of DNA binding by the complexes. Viscosity measurements are very sensitive to length change and are a critical test of the binding model in solution. A significant increase in the viscosity of DNA on addition of any external species can result only when there is intercalation, as the intercalation leads to the separation among the DNA bases and hence an increase in the effective size of DNA which could be the reason for the increase in viscosity [63]. However, in the present case the decrease in the DNA solution viscosity is attributed to the binding between the complex ion and DNA through charge affinity or groove binding, which leads to a destruction of the DNA structure. Partial/non-classical intercalation of a drug molecule could bend the DNA helix, that reduces its effective length and hence its viscosity. The binding of the complex with DNA could be by a surface or groove binding mode. A plot of $(\eta/\eta_0)^{1/3}$ versus [complex]/[DNA] gives a measure of the viscosity changes (Fig. 5a). A marginal decrease of the relative viscosity was observed on addition of complex to DNA, suggesting mainly the groove binding nature of the complexes [64]. The decrease in viscosity may be due to the perturbation of the structural network of DNA caused by binding of the complex molecule.

The nature of the binding of the complexes to CT-DNA was further investigated by DNA melting experiment. DNA melting is observed when ds DNA molecules are heated and separated into two single strands; it occurs due to a disruption of the intermolecular forces, such as π stacking and hydrogen bonding interactions, between DNA base pairs. The DNA melting experiment revealed that the melting temperature of CT-DNA was 69.3 ± 0.2 °C and 70.5 ± 0.2 °C in the absence and presence of **2** respectively. However, for the individual ligands, there is no considerable change in the DNA melting temperature. The DNA denaturation experiment showed only a minor shift in the melting temperature (T_m), giving a ΔT_m value of 1.2 °C on addition of **2** to CT-DNA (Fig. 5b). The low value of ΔT_m suggests primarily a groove-binding preference of the complex to DNA.

3.4. Chemical nuclease activity

DNA cleavage activity of the complexes in the presence of MPA (500 μM) has been investigated using plasmid SC pUC19 DNA (30 μM, 0.2 μg) in 50 mM Tris–HCl buffer/50 mM NaCl (pH 7.2). The extent of DNA cleavage was observed by agarose gel electrophoresis. A 2 μM concentration of **2** completely cleaves SC-DNA into its nicked circular (NC) form in the presence of 500 μM MPA (Fig. 6 and Table 3). Control experiments using SC pUC19 DNA were carried out to study the mechanistic pathway. MPA (500 μM) or the complexes individually do not show any apparent cleavage of SC-DNA under similar reaction conditions (Table 3). The reaction of SC-DNA with copper (II) salts in the presence of MPA does not exhibit any cleavage activity. All the control results suggest that the complexes are responsible for the chemical nuclease activity. The mechanism for the chemical nuclease activity of the complexes was investigated in the presence of various quenchers for reactive oxygen species. Addition of hydroxyl radical scavengers, viz. DMSO, KI or catalase, significantly inhibits the cleavage, so the formation of a hydroxyl (˙OH) radical during the redox reaction involving the copper (II) center in the presence of MPA is a possibility. On the contrary, singlet oxygen scavengers like NaN_3 or TEMP (2,2,6,6-tetramethylpiperidine) do not show any appreciable inhibitory effect on the chemical nuclease activity

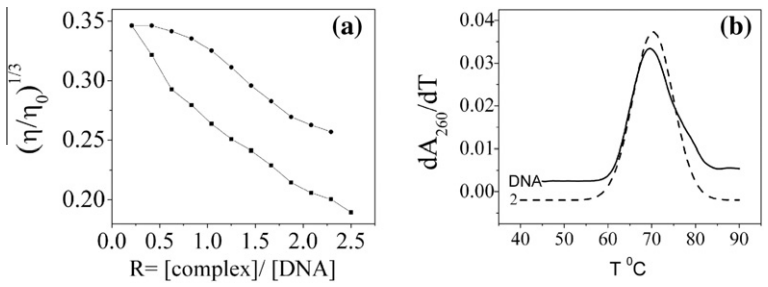

Fig. 5. (a) Effect of increasing amounts of the complexes [Cu(L-orn)(bpy)(Cl)] (**1**) (■) and Cu(L-orn)(phen)(Cl)] (**2**) (●)] on the relative viscosities of CT-DNA at 37.0 (±0.1) °C in 5 mM Tris–HCl buffer (pH, 7.2) [DNA] = 150 μM and *R* = [complex]/[DNA]. (b) DNA melting plots for CT-DNA (160 μM NP) in the absence and presence of **2** (20 μM) in 5 mM phosphate buffer (pH 6.8).

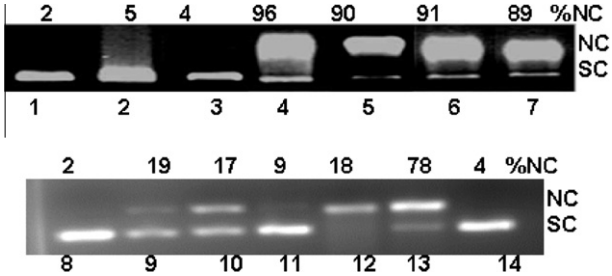

Fig. 6. Gel electrophoresis diagram showing the oxidative cleavage of SC pUC19 DNA (0.2 μg) 30 μM, by the complexes (**1**–**2**) in the presence of 500 μM MPA in 50 mM Tris–HCl/NaCl buffer (pH, 7.2). lane-1, DNA control; lane-2, DNA + MPA; lane-3, DNA + **2** (2 μM); lane-4, DNA + **2** (2 μM) + MPA; lane-5, DNA + **2** (2 μM) + MPA + -methyl green; lane-6, DNA + **2** (2 μM) + MPA + NaN_3; lane-7, DNA + **2** (2 μM) + MPA + SOD; lane-8, DNA + **1** (2 μM); lane-9, DNA + **1** + MPA; lane-10, DNA + **2** + MPA + dist-A; lane-11, DNA + **2** + MPA + catalase; lane-12, DNA + **2** + MPA + DMSO; lane-13, DNA + **2** + MPA + TEMP; lane-14, DNA + MPA + ornithine.

Table 3
Selected DNA cleavage data for the complexes **1** and **2**.

Sl. No.	Reaction conditions	% SC	% NC
1	DNA control	98	2
2	DNA + MPA	95	5
3	DNA + **2**	96	4
4	DNA + **2** + MPA	4	96
5	DNA + **2** + MPA + methyl green	10	90
6	DNA + **2** + MPA + NaN_3	9	91
7	DNA + **2** + MPA + SOD	11	89
8	DNA + **1**	98	2
9	DNA + **1** + MPA	81	19
10	DNA + **2** + MPA + dist. A	83	17
11	DNA + **2** + MPA + catalase	91	9
12	DNA + **2** + MPA + DMSO	82	18
13	DNA + **2** + MPA + TEMP	22	78
14	DNA + **2** + MPA + ornithine	96	4

[Complex] = 2 μM; [MPA] = 500 μM. DMSO = 6 μL. Catalase = 2 unit. SOD = 2 unit. [NaN_3] = 200 μM. [TEMP] = 200 μM. [dist.-A] = 100 μM.

Table 4
IC_{50} values for the complexes (**1**–**2**) against A-549 and HEp-2 cell lines.

Complex	Cell lines	
	A-549 μg/mL (μM)	HEp-2 μg/mL (μM)
[Cu(om)(bpy)(Cl)]Cl·$2H_2O$ (**1**)	9.50 (20.1)	10.0 (22.08)
[Cu(om)(phen)(Cl)]Cl·$2H_2O$ (**2**)	1.15 (2.38)	0.60 (1.24)
[a]Cisplatin	0.45 (1.5)	28.2 (94)
[a]Taxol	4.50 (5.27)	–

Each value represents the mean of three trials.
[a] Positive control.

of **2**. The DNA cleavage activity of the complexes in the presence of MPA probably proceeds through the hydroxyl radical pathway. To determine the groove selectivity of the complexes, control experiments were performed using the minor groove binder distamycin A and the major groove binder methyl green. The presence of methyl green does not inhibit the DNA cleavage and the presence of distamycin A significantly inhibits the DNA cleavage, suggesting the minor groove binding propensity of **2** to the ds DNA.

4. Cytotoxicity assay

4.1. Cytotoxicity of copper (II) complexes of ornithine

A-549 and HEp-2 cells were cultured in the presence of varying concentrations of the copper (II) complexes of ornithine for 1 h and

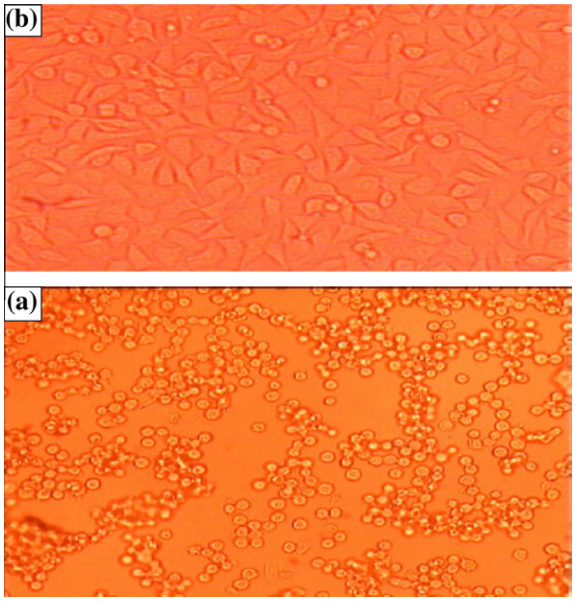

Fig. 7. Morphological changes after treating **2** with HEp-2 cells after an incubation period of 1 h. (a) Normal HEp-2 cell (b) targeted HEp-2 cells after 1 h.

the cytotoxicity was analyzed by sulforhodamine B (SRB) assay. Cisplatin and Taxol were used as a positive control. The IC_{50} values for all the compounds were determined and are given in Table 4. Complex **2** has an IC_{50} value of 1.15 μg/mL (taxol, 4.5; cisplatin, 0.45 μg/mL) and 0.60 μg/mL (cisplatin, 28.2 μg/mL) against A-549 and HEp-2 cells respectively. All the other appropriate ligands and the metal salt used in the synthesis were tested and they had no considerable IC_{50} values. The morphological changes in the HEp-2 cell lines after treatment with **2** are shown in Fig. 7.

5. Antimicrobial activity

The antimicrobial activities of **1**, **2**, the ligands and the copper salt were evaluated against a panel of pathogenic bacterial strains by the disc diffusion and serial dilution method in aqueous medium. MIC values (μg/mL) for **1**, **2**, bpy and phen are summarized in Table 5. The ionic complexes of the transition metal interfere with the transport of substrates and ions through the cell membrane, resulting in antibacterial activity. The results indicate that complex **1** exhibits relatively high antibacterial activity against *S. mutans* and *P. vulgaris* compared to its ligands and **2**. On chelation, the polarity of the metal ion will be reduced to a greater extent due to the overlapping of the ligand orbital and the partial sharing of the positive charge of the metal ion with the donor groups. Further, it increases the delocalization of π-electrons over the whole chelate ring and enhances the lipophilicity of the complexes. This increased lipophilicity enhances the penetration of the complexes

Table 5
Minimum inhibitory concentration for the complexes (**1**–**2**) and the ligands μg/mL (mM).

Bacterial strains	**1**	**2**	bpy	phen
B. subtilis	475 (1.01)	–	–	450 (2.50)
M. luteus	325 (0.67)	500 (3.2)	500 (3.2)	1000 (5.50)
S. aureus	2000 (4.14)	–	–	2000 (11.10)
S. mutans	250 (0.51)	1000 (6.4)	1000 (6.4)	1000 (5.50)
E. coli	350 (0.72)	–	–	500 (2.75)
P. aeruginosa	250 (0.51)	–	–	1000 (5.50)
P. vulgaris	275 (0.57)	–	–	1000 (5.50)

into lipid membranes, interferes with enzyme activity and may lead to cell apoptosis. The antifungal activity against *Candida albica* for **1**, **2** and the ligands was investigated, and considerable activity was not observed under the assay conditions.

6. Conclusion

Two new ternary copper (II) complexes having *N*,*O*-donor L-ornithine and *N*,*N*-donor heterocyclic base (B) are prepared and structurally characterized. The planarity and extended conjugation of the phenanthroline ligand have a profound effect on the DNA binding and cleavage activity of the complexes. Complex **2** shows efficient chemical nuclease activity in the presence of MPA. Pathways involving hydroxyl radicals in the DNA cleavage reactions are proposed from control studies, which show inhibition of the cleavage in the presence of the hydroxyl radical scavengers DMSO, catalase and KI. The long aliphatic chain with a terminal positive pendant of the ornithine complex may marginally enhance the DNA cleavage activity. The DNA cleavage activity of transition metal complexes with bio-essential constituents like copper and active amino acids showing DNA cleavage have the potential for cellular applications in chemotherapeutic agents. Complex **2** has promising anticancer activity against HEp-2 cell lines. Complex **1** is an active antibacterial agent against *S. mutans* and *P. aeruginosa*.

Acknowledgments

Financial support received from the Department of Science and Technology (DST, SR/S5/BC-14/2006), Government of India, is gratefully acknowledged. The authors gratefully acknowledge the support of Prof. A. R. Chakravarty, Department of Inorganic and Physical Chemistry, Indian Institute of Science, Bangalore, India, in providing facilities and useful discussions. R.K. is thankful to DST for a fellowship.

Appendix A. Supplementary data

Detailed crystallographic data for the structural analysis, giving atomic coordinates, thermal parameters and structure refinement parameters, have been deposited with the Cambridge Crystallographic Data Centre. CCDC 803869 contains the supplementary crystallographic data for **2**. These data can be obtained free of charge via http://www.ccdc.cam.ac.uk/conts/retrieving.html, or from the Cambridge Crystallographic Data Centre, 12 Union Road, Cambridge CB2 1EZ, UK; fax: (+44) 1223-336-033; or e-mail: deposit@ccdc.cam.ac.uk.

References

[1] (a) A. Korfel, M.E. Scheulen, H.J. Schmoll, O. Grundel, A. Harstrick, M. Knoche, L.M. Fels, M. Skorzec, F. Bach, J. Baumgart, G. Sab, S. Seeber, E. Thiel, W. Berdel, Clin. Cancer Res. 4 (1998) 2701;
(b) C.V. Christodoulou, D.R. Ferry, D.W. Fyfe, A. Young, J. Doran, T.M.T. Sheehan, A. Eliopoulos, K. Hale, J. Baumgart, G. Sass, D.J. Kerr, J. Clin. Oncol. 16 (1998) 2761;
(c) D.S. Sigman, T.W. Bruice, A. Mazumder, C.L. Sutton, Acc. Chem. Res. 26 (1993) 98;
(d) M.S. Deshpande, A.A. Kumbhar, A.S. Kumbhar, M. Kumbhakar, Haridas Pal, U.B. Sonawane, R.R. Joshi, Bioconjugate Chem. 20 (2009) 447.
[2] (a) D.S. Sigman, A. Mazumder, D.M. Perrin, Chem. Rev. 93 (1993) 2295;
(b) G. Gilles, I. Ott, N. Metzler-Nolte, J. Med. Chem. 54 (2011) 3.
[3] (a) B. Meunier, Chem. Rev. 92 (1992) 1411;
(b) Yi Shi, B.B. Toms, N. Dixit, N. Kumari, L. Mishra, J. Goodisman, J.C. Dabrowiak, Chem. Res. Toxicol. 23 (2010) 1417;
(c) S. Sandipan, S. Supriti, D. Sourav, Z. Ennio, P. Chattopadhyay, Polyhedron 29 (2010) 3157.
[4] (a) G. Pratviel, J. Bernadou, B. Meunier, Adv. Inorg. Chem. 45 (1998) 251;
(b) G. Pratviel, J. Bernadou, B. Meunier, Angew. Chem., Int. Ed. Engl. 34 (1995) 746.
[5] (a) W.Y. Lee, Y.K. Yan, P.P.F. Lee, S.J. Tan, K.H. Lim, Metallomics 4 (2012) 188;
(b) T. Bortolotto, P.P. Silva, A. Neves, E.C. Pereira-Maia, H. Terenzi, Inorg. Chem. 50 (2011) 10519.
[6] (a) C. Metcalfe, J.A. Thomas, Chem. Soc. Rev. 32 (2003) 215;
(b) A. Arnau, F. Marc, M.M. Angeles, F. Xavier, P.M. Jose, M. Virtudes, S. Xavier, L. Antoni, Inorg. Chem. 48 (2009) 11098.
[7] (a) B.S. Creaven, B. Duff, D.A. Egan, K. Kavanagh, G. Rosair, V.R. Thangella, M. Walsh, Inorg. Chim. Acta 363 (2010) 4048;
(b) B.A.J. Jansen, J.M. Pérez, A. Pizarro, C. Alonso, J. Reedijk, C.N. Ranninger, Inorg. Biochem. 85 (2001) 229.
[8] (a) A. Hussain, S. Gadadhar, T.K. Goswami, A.A. Karande, A.R. Chakravarty, Eur. J. Med. Chem. 50 (2012) 319;
(b) A. Hussain, S. Gadadhar, T.K. Goswami, A.A. Karande, A.R. Chakravarty, Dalton Trans. 41 (2012) 885;
(c) S. Dhar, A.R. Chakravarty, Inorg. Chem. 42 (2003) 2483.
[9] (a) B. Armitage, Chem. Rev. 98 (1998) 1171;
(b) T. Rosu, E. Pahontu, C. Maxim, R. Georgescu, N. Stanica, A. Gulea, Polyhedron 30 (2011) 154.
[10] D.R. McMillin, K.M. McNett, Chem. Rev. 98 (1998) 1201.
[11] H.T. Chifotides, K.R. Dunbar, Acc. Chem. Res. 38 (2005) 146.
[12] E.R. Jamieson, S.J. Lippard, Chem. Rev. 99 (1999) 2467.
[13] K.S. Asprazak, Chem. Res. Toxicol. 4 (1991) 604.
[14] (a) T.D. Tullius, in: Metal–DNA Chemistry, ACS Symposium Series, vol. 402, American Chemical Society, Washington, DC, 1989;
(b) M.E. Vahter, in: T.W. Clarkson, L. Friberg, G.F. Nordberg, P.R. Sanger (Eds.), Biological Monitoring of Toxic Metals, Plenum, New York, 1988, p. 303.
[15] (a) S.J. Lippard, J.M. Berg, in: Principles of Bioinorganic Chemistry, University Science Books, Sausalito, CA, 1994.
[16] (a) H. Umezawa, Prog. Biochem. Pharmacol. 11 (1976) 18;
(b) Z.H. Chohan, H.A. Shad, M.H. Youssoufi, B.T. Hadda, Eur. J. Med. Chem. 45 (2010) 2893.
[17] R.M. Burger, Chem. Rev. 98 (1998) 1153.
[18] B.M. Zeglis, V.C. Pierre, J.K. Barton, Chem. Commun. (2007) 4565.
[19] T.K. Janaratne, A. Yadav, F. Ongeri, F.M. MacDonnel, Inorg. Chem. 46 (2007) 3420.
[20] S. Delaney, M. Pascaly, P.K. Bhattacharya, K. Han, J.K. Barton, Inorg. Chem. 41 (2001) 1966.
[21] K.E. Erkkila, D.T. Odom, J.K. Barton, Chem. Rev. 99 (1999) 2777.
[22] (a) A. Sitlani, E.C. Long, A.M. Payle, J.K. Barton, J. Am. Chem. Soc. 114 (1992) 2303;
(b) L. Tjioe, T. Joshi, J. Brugger, B. Graham, L. Spiccia, Inorg. Chem. 50 (2011) 621;
(c) S.S. Bhat, A.A. Kumbhar, H. Heptullah, A.A. Kahn, V.V. Gobre, S.P. Gejji, V.G. Puranik, Inorg. Chem. 50 (2011) 545.
[23] C.J. Burrows, J.G. Muller, Chem. Rev. 98 (1998) 1109.
[24] W.K. Pogozelski, T.D. Tullius, Chem. Rev. 98 (1998) 1089.
[25] A.K. Patra, M. Nethaji, A.R. Chakravarty, Dalton Trans. (2005) 2798.
[26] A.K. Patra, S. Dhar, M. Nethaji, A.R. Chakravarty, Dalton Trans. (2005) 896.
[27] A.K. Patra, T. Bhowmick, S. Ramakumar, M. Nethaji, A.R. Chakravarty, Dalton Trans. (2008) 6966.
[28] A.K. Patra, S. Dhar, M. Nethaji, A.R. Chakravarty, Chem. Commun. (2003) 1562.
[29] P.K. Sasmal, R. Majumdar, R.R. Dighe, A.R. Chakravarty, Dalton Trans. 39 (2010) 7104.
[30] (a) F. Arjmand, B. Mohani, S. Ahmad, Eur. J. Med. Chem. 40 (2005) 1103;
(b) M.N. Patela, P.A. Dosia, B.S. Bhatta, V.R. Thakkar, Spectrochim. Acta, Part A 78 (2011) 763.
[31] P.K. Sasmal, A.K. Patra, M. Nethaji, A.R. Chakravarty, Inorg. Chem. 46 (2007) 11112.
[32] S. Dhar, D. Senapati, P.A.N. Reddy, P.K. Das, A.R. Chakravarty, Chem. Commun. (2003) 2452.
[33] A.K. Patra, T. Bhowmick, S. Roy, A.R. Chakravarty, Inorg. Chem. 48 (2009) 2932.
[34] M. Roy, T. Bhowmick, S. Ramakumar, M. Nethaji, A.R. Chakravarty, Dalton Trans. (2008) 3542.
[35] P.K. Sasmal, S. Saha, R. Majumdar, R.R. Dighe, A.R. Chakravarty, Inorg. Chem. 49 (2010) 849.
[36] (a) M.S.A. Begum, S. Saha, M. Nethaji, A.R. Chakravarty, Indian J. Chem. 48A (2009) 473;
(b) A.K. Patra, T. Bhowmick, S. Ramakumar, A.R. Chakravarty, Inorg. Chem. 46 (2007) 9030.
[37] R.K. Rao, A.K. Patra, P.R. Chetana, Polyhedron 26 (2007) 5331.
[38] R.K. Rao, A.K. Patra, P.R. Chetana, Polyhedron 27 (2008) 1343.
[39] P.R. Chetana, R.K. Rao, M. Roy, A.K. Patra, Inorg. Chim. Acta 362 (2009) 4692.
[40] A.L. Lehninger, Biochemistry, Worth Publishers Inc., New York, 1970. p. 69.
[41] A.C. Kurtz, J. Biol. Chem. 180 (1949) 1253.
[42] R. Roeske, F.H.C. Stewart, R.J. Stedman, V. du Vigneaud, J. Am. Chem. Soc. 78 (1956) 5883.
[43] (a) J.G. Skinner, J. Johansson, Med. Chem. 15 (1972) 427;
(b) A.B.P. Lever, E. Mantovani, Inorg. Chem. 10 (1971) 817.
[44] D.H. Russell, S.H. Snyder, Fed. Proc. Fed. Am. Soc. Exp. Biol. 27 (1968) 642.
[45] D.H. Russell, S.H. Snyder, Proc. Natl. Acad. Sci. USA 60 (1968) 1420.
[46] D.D. Perrin, W.L.F. Armarego, D.R. Perrin, Purification of Laboratory Chemicals, Pergamon Press, Oxford, 1980.
[47] O. Khan, Molecular Magnetism, VCH, Weinheim, 1993.
[48] (a) G.M. Sheldrick, SADABS, Program for Empirical Absorption Correction, University of Göttingen, Germany, 1996;
(b) Bruker, SADABS, Bruker AXS Inc., Madison, WI, USA, 2001.

[49] G.M. Sheldrick, SHELX-97, Program for Crystal Structure Solution and Refinement, University of Gottingen, Gottingen, Germany, 1997.
[50] C.K. Johnson, ORTEP-III, Report ORNL – 5138, Oak Ridge National Laboratory, Oak Ridge, TN, 1976.
[51] J. Marmur, J. Mol. Biol. 3 (1961) 208.
[52] M.E. Reichmann, S.A. Rice, C.A. Thomas, P. Doty, J. Am. Chem. Soc. 76 (1954) 3047.
[53] J.D. McGhee, P.H. von Hippel, J. Mol. Biol. 86 (1974) 469.
[54] M.T. Carter, M. Rodriguez, A.J. Bard, J. Am. Chem. Soc. 111 (1989) 8901.
[55] M.J. Waring, J. Mol. Biol. 13 (1965) 269.
[56] J.B. LePecq, C. Paoletti, J. Mol. Biol. 27 (1967) 87.
[57] M. Lee, A.L. Rhodes, M.D. Wyatt, S. Forrow, J.A. Hartley, Biochemistry 32 (1993) 4237.
[58] J. Bernadou, G. Pratviel, F. Bennis, M. Girardet, B. Meunier, Biochemistry 28 (1989) 7268.
[59] (a) W. Voigt, Mol. Med. 110 (2005) 39;
(b) R. Subramanian, Z.M. Asmawi, A. Sadikun, V. Vichai, K. Kirtikara, Nat. Protoc. 1 (2006) 112;
(c) V. Vijayan, S. Vinod Kumar, S.A. Dhanaraj, S. Badami, B. Suresh, Pharm. Biol. 40 (2002) 456.
[60] P.K. Mukherjee, R. Balasubramanian, K. Saha, B.P. Saha, M. Pal, Indian Drugs 32 (1995) 274.
[61] R.N. Jones, A.L. Barry, T.L. Gavan, J.A.I. Washington, Microdilution and macrodilution broth procedures, in: E.H. Lennette, A. Balows, W.J. Hausler Jr., H.J. Shadomy (Eds.), Manual of Clinical Microbiology, American Society for Microbiology, Washington, DC, 1985, p. 972.
[62] R.B. Nair, E.S. Teng, S.L. Kirkland, C.J. Murphy, Inorg. Chem. 37 (1998) 139.
[63] S. Satyanarayana, J.C. Dabrowiak, J.B. Chaires, Biochemistry 32 (1993) 2573.
[64] J.E. Coury, J.R. Anderson, L. McFail-Isom, L.D. Williams, L.A. Bottomley, J. Am. Chem. Soc. 119 (1997) 3792.